ARMA 15-254

Contribution of shear slip in a widespread compressive pillar failure

Poeck, E.
Garvey, R.
Zhang, K.
Ozbay, U.
Colorado School of Mines, Golden, CO, USA

This paper was prepared for presentation at the 49th US Rock Mechanics / Geomechanics Symposium held in San Francisco, CA, USA, 28 June-1 July 2015.

ABSTRACT: A release of energy occurs during mining-related seismic events such as rock bursts and coal bumps. The magnitude of these events depends partly upon the energy made available by the loading system and partly upon the post-peak softening behavior of the failing medium. In addition, the extent of unstable failure and associated release of energy can be affected by slip along interfaces between dissimilar materials. This paper compares the results of two numerical models from the back analysis of a coal mine collapse which resulted in a 3.9 local magnitude seismic event. Release of kinetic energy is considered in the simulations, which were run using a 2D distinct element software package. The model inputs differ in that the interfaces between the coal and the surrounding rock are defined either through Coulomb slip joint parameters or continuously yielding (displacement-softening) joint parameters. The geometry, loading conditions, and mining sequence are otherwise identical. The coal is modeled as a strain-softening material, while the roof and floor are modeled as continuous elastic blocks. The failure response and magnitude of released energy are compared between the two models. The results of the analysis indicate that the softening coal/rock interface facilitates the collapse of large width-to-height ratio pillars and leads to a release of energy more than one order of magnitude higher than the alternative coal-rock interface.

1. INTRODUCTION

The unstable failure of coal pillars, especially those with large width-to-height (w/h) ratios, involves a great deal of complexity. Although large w/h pillars exhibit hardening behavior under loading and are prone to fail gradually, the combination of certain loading conditions and geologic properties can result in sudden collapse. The nature and extent of such failures depends on many factors, including the geometry of the mine and the presence of stiff overlying strata. Another factor that has a significant effect on the behavior of the pillars is the strength, or rather weakness, of the interface between the coal and the host rock. There is little data available regarding the properties of coal/rock interfaces, but a number of studies have been conducted to better understand the effect that they have on pillar strength [1], [2], [3], and [4]. This paper presents the results of two mine-scale numerical models in which a pillar retreat mine fails unstably, and although the modeling procedures are identical in each simulation, the application of different coal/rock interface parameters results in a different progression and magnitude of failure.

The models presented here are part of a back-analysis of the collapse of the Crandall Canyon coal mine, wherein a large number of pillars failed violently and near-simultaneously. Information regarding the series of events and conditions at the time of the failure can be found within the Mine Safety and Health Administration (MSHA) accident report [5]. In this study, the unstable failure of the Main West section of the mine is reproduced in the two-dimensional distinct element code UDEC [6] and the magnitude of unstable failure is quantified by calculating the kinetic energy released during mining. The average vertical stress and strain measured across the width of various pillars shows a clear difference in peak and residual strengths when different interface parameters are used. Additionally, closure profiles of the coal seam at various stages of the simulation illustrate large discrepancies in the predicted outcome of the mining sequence. Both of the models presented in this paper used Mohr-Coulomb strain-softening (MCSS) properties in the coal seam. A comparison is made between the Coulomb slip joint

(CS) and the Continuously-Yielding joint (CY) in the coal/rock interface.

An overview of the study is given in the following sections, which include the assumptions and input parameters used in the modeling approach and a discussion of energy calculations. Results are presented for key topics, including pillar failure mechanisms and response of the mine-scale models, followed by the conclusions of the analysis.

2. MODELING APPROACH

The model constructed for this analysis represents a 2D, north-south cross section through the entire Main West section of the mine, with a 4-meter thick coal seam and an overburden depth of 609 meters. The model is shown in Figure 1. The top of the model is a free surface, the bottom is fixed in the vertical direction, and the left and right boundaries of the model are fixed in the horizontal direction. The coal/rock interfaces are explicitly modeled both above and below the coal seam. The material above and below the coal seam is modeled as an elastic medium. The continuous overburden forces the system of pillars across the coal seam to work simultaneously against the roof as changes to the excavation geometry and loading conditions progress. This approach was adopted because of the presence of stiff overburden units at the mine and the nature of the collapse, in which a large number of pillars failed together [5].

2.1. Abutment Loading

Abutment loads from the longwall panels to the north and south of the Main West (MW) area were a significant factor in the loading conditions at the time of the collapse. These abutment loads are simulated through the use of grid point forces along the right and left boundaries. An abutment angle of 21 degrees was assumed for normal caving conditions, as suggested in the Analysis of Retreat Mining Pillar Stability (ARMPS) program [7]. The vertical distribution of applied abutment forces was developed through a separate model which treated the abutment triangle as an elastic wedge under gravitational loading. Comparisons between the abutment load transfer distance within the models and those revealed by a recent instrumented longwall study in a deep western U.S. coal mine [8] showed similar results.

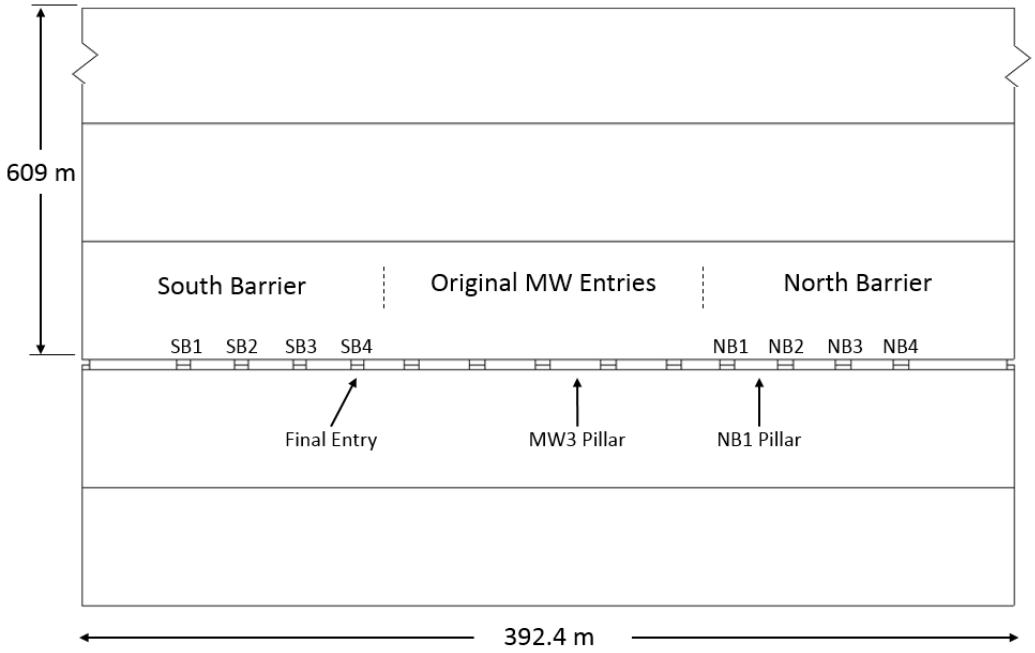

Figure 1. 2D model of Crandall Canyon Main West

2.2. Material Properties

A thorough calibration of material properties was performed before execution of the mine-scale models. In this process, a series of individual pillar models with varying w/h ratios were failed under compression to ensure that their peak or nominal strength was consistent with the predicted strength of similarly-sized coal pillars [9] and [10]. These tests were performed with a fixed interface between the coal and rock. The material properties of the coal and overburden used in the mine-scale simulations are shown in Table 1. The Mohr-Coulomb strain softening parameters used for coal are shown in Table 2.

Table 1: Material properties used in mine-scale simulations

Material	Density (kg / m^3)	Young's Mod. (Pa)	Poisson Ratio	Friction Angle (deg)	Cohesion (Pa)	Dilation Angle (deg)	Tensile Strength (Pa)
Overburden	2350	23.4e9	0.26	-	-	-	-
Coal	1313	3.0e9	0.20	23.0	1.69e6	2.0	0.0

Table 2: Softening parameters used in coal

Cohesion (Pa)		Friction Angle (deg)		Dilation angle (deg)	
0.00000	1.69E+06	0.00000	23	0.00000	2
0.00006	1.54E+06	0.00007	27.5	0.00007	10
0.00008	1.47E+06	0.00010	30	0.01360	10
0.03500	2.00E+05	1.00000	30	0.01413	2
1.00000	2.00E+05			1.00000	2

Coal/rock interface property calibration was performed prior to the study. A friction angle of 20 degrees and cohesion of zero were selected for the Coulomb slip interface. This friction angle lies within the range of 10 to 25 degrees suggested for fault gouge and smooth rock surfaces respectively [2]. The shear stress / shear displacement graphs for each of the CS and CY joint constitutive models is shown in Figure 2, and the joint parameters are shown in Table 3.

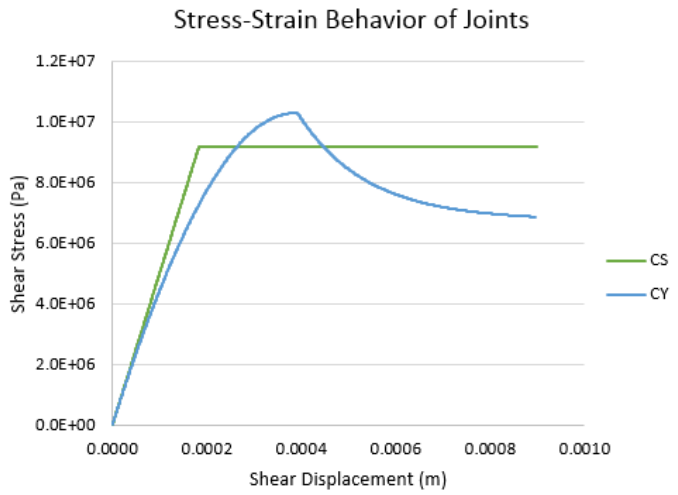

Figure 2. Shear stress / shear strain curves of joints used in coal/rock interfaces

Table 3. Properties of joints used in coal/rock interfaces

	Coulomb Slip	Continuously Yielding
Shear Stiffness (Pa)	50.0e9	50.0e9
Normal Stiffness (Pa)	50.0e9	50.0e9
Initial Friction angle (deg)	20.0	40.0
Intrinsic Friction angle (deg)	-	15.0
Joint roughness (m)	-	0.00015
Cohesion (Pa)	0.0	-
Dilation angle (deg)	0.0	-
Tensile Strength (Pa)	0.0	-

2.3. Excavation Sequence

Each excavation (mine entry) was divided into vertical slices 0.4 meters wide and mined one slice at a time from left to right. Furthermore, each slice was deleted and replaced with equivalent reaction forces, which were reduced over 100 increments to avoid potential dynamic effects of simulated mining. On the mine scale, the excavations and abutment loads were developed in the following general order:

I. Excavation of Main West entries 1 – 5
II. Abutment load on south boundary of model
III. Abutment load on north boundary of model
IV. Excavation of entries 1 – 4 in north barrier
V. Retreat mining of two pillars in north barrier
VI. Excavation of entries 1 – 4 in south barrier

3. ENERGY CALCULATION

A significant aspect of this study involved the calculation of released energy for a direct comparison of the magnitude of failures that took place in different models. The UDEC software package provides an energy calculation procedure and records several energy terms in individual histories. The value of released energy is governed by the following equation [6]:

$$W_r = U_k + W_k + W_v + U_m \quad (1)$$

Where:
W_r is the total released energy
U_k is current value of kinetic energy in the system
W_k is the total work dissipated by mass damping
W_v is the work done by viscous boundaries (not applicable in this study)
U_m is the total strain energy in excavated material

This equation was modified to eliminate terms that are not applicable when comparing model results. The work done by viscous boundaries, W_v, is zero because the models in this study do not have viscous boundaries. Additionally, the strain energy of mined material, U_m, was excluded from released energy totals. Thus, the total released energy during the simulation is accounted for by the equation:

$$W_r = U_k + W_k \quad (2)$$

Comparison of W_r values between different mine-scale models provides a scalar measure of the unstable failures that take place, while plots of the changes in kinetic energy indicate when unstable failures occur.

4. FAILURE OF A PILLAR

This section describes the difference in strength of a single pillar from the mine-scale models with either Coulomb Slip (CS) or Continuously-Yielding (CY) coal/rock interface parameters. The MW3 pillar is considered here, which is located near the center of the model shown in Figure 1. The behavior of the pillar is compared between two states: 1) when two of four entries have been developed in the North Barrier, and 2) when three of four entries have been developed in the North Barrier.

Figure 3 shows stress/strain of the MW3 pillar before and after excavation of the third entry in the North Barrier. Note that very little increase in stress occurs in the model with the CS interface while development of the third entry produces pillar failure with the CY interface. It is worth noting that the pillar bound by the CS interface exhibits hardening behavior throughout the time period considered in this study, eventually reaching a stress value of 34 MPa

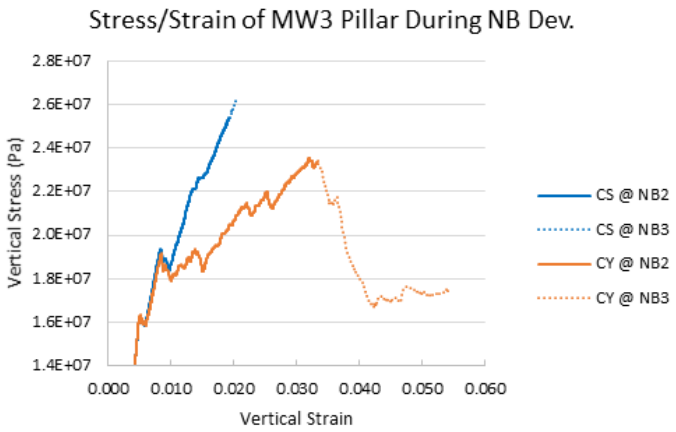

Figure 3. Stress/strain of MW3 pillar before and after development of third entry in North Barrier. Results shown for two models with different coal/rock interface properties.

Figure 4 shows the distribution of vertical stresses at mid height of the MW3 pillar before and after the third entry is developed. The Coulomb slip interface provides confinement closer to the ribs that allows vertical stress to be sustained across a larger interior portion of the pillar. The CY coal/rock interface promotes a larger yield zone at the perimeter of the pillar and forces a higher concentration of stress at the core. These two modes of pillar behavior, dependent upon shear confinement in the coal/rock interface, were conceptualized by Gale [3] in a study of pillar strength and surrounding strata properties.

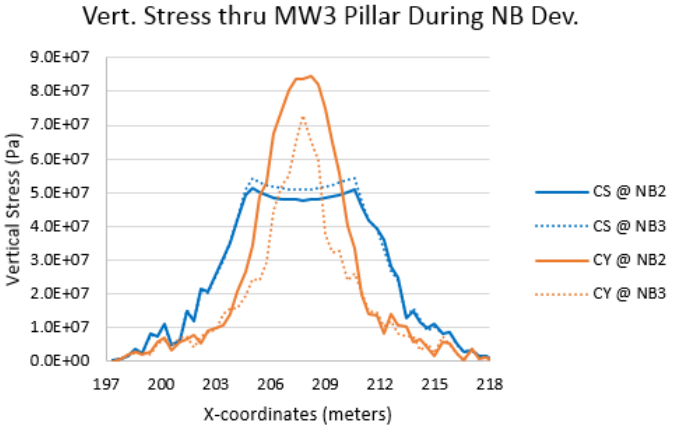

Figure 4. Distribution of vertical stress, at different stages of excavation, through pillars with differing coal/rock interface properties

Figure 4 also shows that the high-stress core of the pillar with the CY interface reduces in width and load-bearing capacity during failure. Successive loading on this pillar will induce softening along portions of the coal/rock

interface closer to the core, promoting additional horizontal displacement near the ribs, and further de-confinement and softening of the core. The potential for unstable pillar failure is tied to the stiffness of the loading system, meaning that sudden failure of the pillar will occur if the roof, or a portion of the roof, becomes capable of large sudden displacements.

5. RESULTS

This section contains results of the mine-scale numerical models for two different phases of mining in the Main West section including: 1) development of the North Barrier with discussion of energy release and pillar deformation, and 2) development of the South Barrier with discussion of energy release and the evidence of a collapse event.

5.1. Development of North Barrier

The development of entries in the north barrier reveals a significant difference between the models with Coulomb slip and Continuously-Yielding coal/rock interface properties. Plots of kinetic energy release are shown in Figure 5, with results of the CS interface model shown in blue and the CY model shown in orange. The x-axis represents a scale of simulation time, which is a function of the time step used in calculations and the number of time steps that have been executed. The value of simulation time has no physical significance, as some models require more computation time than others. Note that the magnitude of kinetic energy spikes is relatively small, typically in the range of tens of thousands of Joules for both the CS and CY interface models. The size of the energy spikes indicates that the softening interface between the coal and rock facilitates individual failure events of greater magnitude.

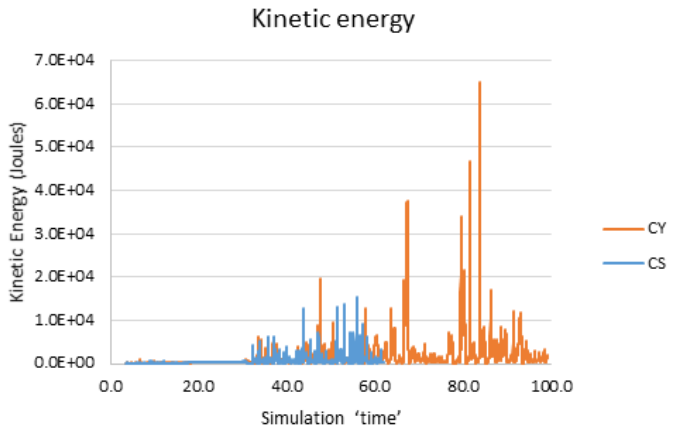

Figure 5. Kinetic energy release during development of NB

Figure 6 shows the accumulation of released energy throughout development of the North Barrier. The stepped features in the lines indicate small instances of instability, which correspond to spikes of various sizes in the kinetic energy plot. The difference in overall size of the lines illustrates that the softening coal/rock interface results in a significantly greater release of energy.

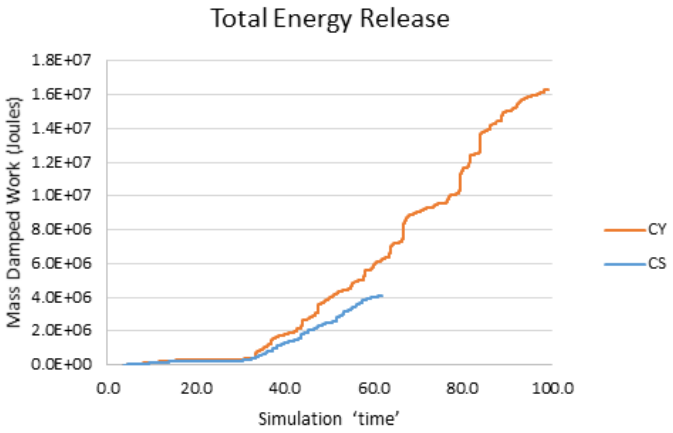

Figure 6: Total released energy during development of NB

The difference in pillar response between the two interface models (CS and CY) is reiterated in Figure 7, which shows the stress/strain behavior of the pillar located between the first two north barrier entries (pillar NB1). See Figure 1 for the location of the pillar.

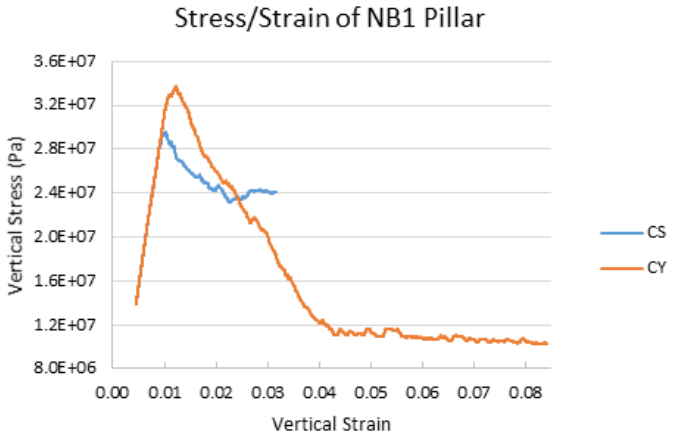

Figure 7: Average vertical stress/strain of NB1 pillar

In this area of the mine, the pillars in both models have failed, but the contribution of the coal/rock interface properties is made evident by the higher peak strength and lower residual strength of the CY model. The pillar bound by a Coulomb Slip interface exhibits a higher residual strength, and the smaller value of vertical strain indicates less closure in the coal seam.

5.2. *Development of South Barrier*

Development of the entries in the South Barrier, particularly the fourth entry, results in a massive failure in the model with softening coal/rock interface parameters. The magnitude of this failure is evidenced by spikes in the plot of kinetic energy, shown in Figure 8, where the largest spike is in the range of megajoules (MJ).

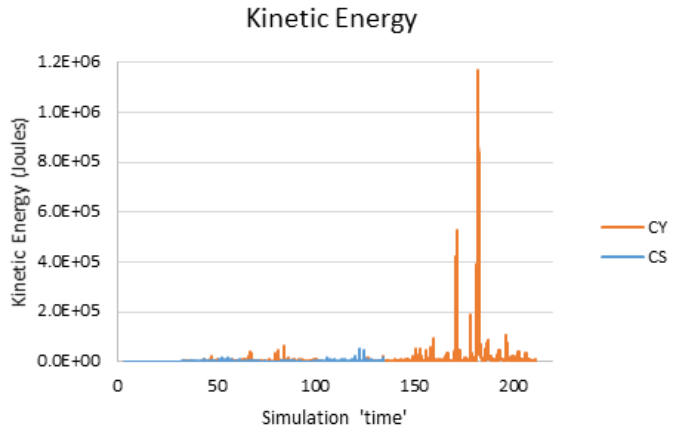

Figure 8: Kinetic energy release after development of SB

Figure 9 shows the cumulative energy released during all stages of development. The graph illustrates a significantly higher release of energy with the use of the Continuously-Yielding parameters in the coal/rock interface, and the large stepped portions of the curve correspond to the magnitude of energy associated with widespread failure.

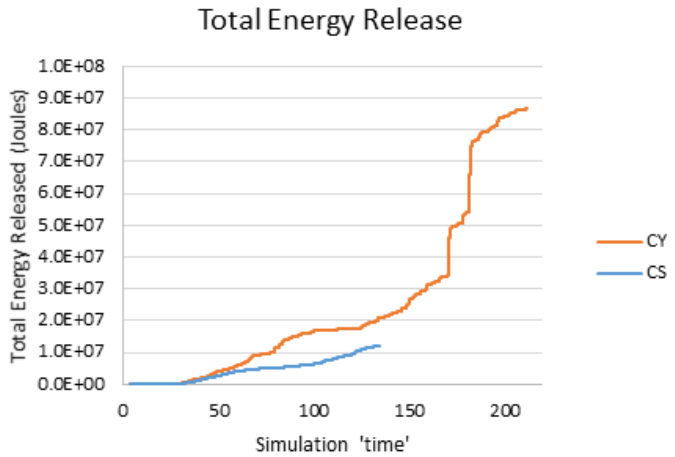

Figure 9: Total released energy during development of SB

The energy of the collapse is better illustrated in Figure 10 with the values of energy released per stage of development in both the North and South Barrier. The graph shows that development of the final entry resulted in the release of approximately 54 MJ with the softening coal/rock interface. The amount of energy released during development of the same entry in the simulation with a CS interface was only 3.2 MJ, signifying a much lesser degree of unstable failure in the coal seam and more than an order of magnitude difference in released energy between the models. Although there was no evidence of widespread pillar failure in the model with the Coulomb slip interface, the development of the final entry still accounted for a significant portion of the released energy in that simulation.

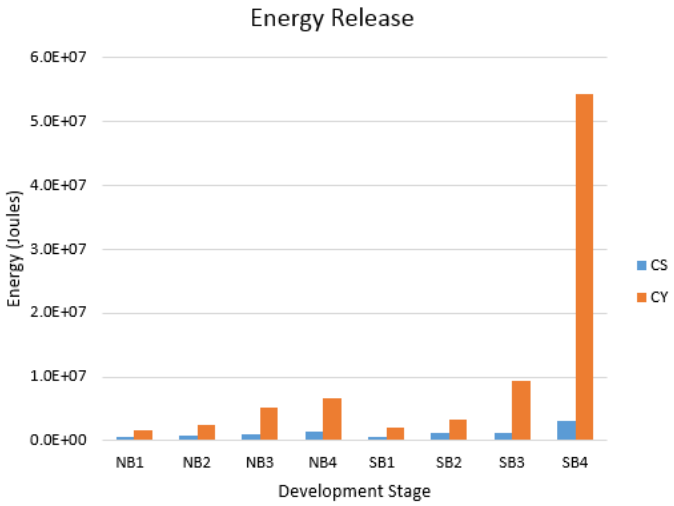

Figure 10: Energy released during each stage of development in NB and SB

Further evidence of the large failure event is provided by the roof displacement contours shown in Figure 11. The graph illustrates the extent of closure in each model before and after development of the four South Barrier entries. Additionally, the graph contains a closure scanline for the state of the CY model in which only three of the last four entries are developed, referred to as SB3. The SB3 line helps illustrate the closure that occurred during development of the final entry. The configuration of pillars and entries present in the final state of the model is shown in the diagram near the top of the graph.

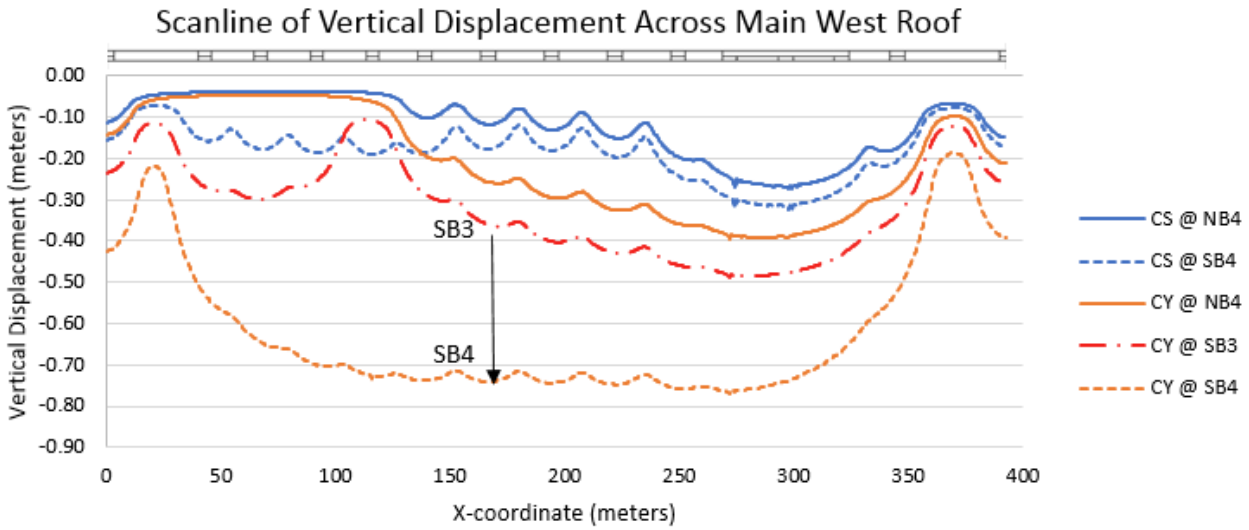

Figure 11: Closure scanlines before and after development of the South Barrier entries

The unstable failure of pillars in the CY model between stages SB3 and SB4 is made evident by the displacements in Figure 11 and the energy released in Figure 10. Development of the SB4 entry subjects the system of pillars across the Main West to loads beyond their collective strength, and the stiff overburden moves downward until resistance is re-established by the remnant barrier pillars in the north and south. The unstable failure of the pillars is attributed to the softening characteristics of the coal and the coal/rock interface as well as the "softness" of the loading system, which refers to the downward displacement of the overburden without obstruction.

6. CONCLUSION

A back-analysis of the Crandall Canyon mine collapse provides an opportunity to assess the effects of various material and coal/rock interface properties on unstable failure. Results of this study reveal that the combination of a strain-softening coal material and a softening coal/rock interface facilitates a progression of pillar failure and sudden collapse in the mine-scale model that correlates well with events at the mine. More importantly, the collapse of the model indicates that the unstable failure of large width-to-height ratio pillars can be simulated while using a range of commonly accepted input parameters.

Consideration of the kinetic energy released during controlled excavation steps helps identify unstable failure events while the total released energy provides a quantitative assessment of their magnitude. Results indicate that a coal/rock interface with softening properties leads to a reduction in strength of individual pillars and a release of energy during the simulated collapse event more than one order of magnitude higher than with Coulomb-slip interface properties. Future analyses of coal pillar strength and failure behavior may benefit from the combined use of softening parameters for material in compression and for bedding plane discontinuities in shear.

7. REFERENCES

1. Babcock, C.O., and D.L. Bickel. Constraint—the missing variable in the coal burst problem. In *Rock Mechanics in Productivity and Protection - Proceedings of the 25th Symposium on Rock Mechanics. Littleton, CO. Society for Mining, Metallurgy, and Exploration, Inc*. 1984.

2. Iannacchione, A.T. The effects of roof and floor interface slip on coal pillar behavior. In *Proceedings of the 31st US Symposium on Rock Mechanics*. 1990.

3. Gale, W.J. Experience of field measurement and computer simulation methods of pillar design. In *Proceedings of the Second International Workshop on Coal Pillar Mechanics and Design. Vail, CO. 1999.* 49-61

4. Lu, J., A. Ray, K. Morsy, and S. Peng. Effects of Rock/Coal Interface Property on Coal Pillar Strength. In *Proceedings of the 27th International Conference on Ground Control in Mining. Morgantown, WV. 2008*.

5. Gates, R., et al. Report of Investigation—Fatal Underground Coal Burst Accidents, August 6 and 16, 2007, Crandall Canyon Mine, Genwal Resources Inc, Huntington, Emery County, Utah." *Department of Labor, Mine Safety and Health Administration, ID* 42-01715. 2008.

6. Itasca Consulting Group. Universal Distinct Element Code (UDEC). Version 5.00. *User's Manual*. 2014

7. Mark, C., and F.E. Chase. Analysis of retreat mining pillar stability (ARMPS). In *Proceedings-New Technology for Ground Control in Retreat Mining. Pittsburgh, PA: US Department of Health and Human Services, Public Health Service, Centers for Disease Control and Prevention, National Institute for Occupational Safety and Health, DHHS (NIOSH) Publication*. No. 97-122. 1997.

8. Larson, M.K., and J.K. Whyatt. "Load Transfer Distance Calibration of a Coal Panel Scale Model: a Case Study." *Proceeding of 31st International Conference on Ground Control in Mining, Morgantown: WV*. 2013

9. Salamon, M.D.G., and A.H. Munro. A study of strength of coal pillars. *Journal of the South African Institute of Mining and Metallurgy*. 1967. 55

10. Mark, C. State-of-the-art in coal pillar design. *TRANSACTIONS-SOCIETY FOR MINING METALLURGY AND EXPLORATION INCORPORATED*. 2000. 123-128.

11. Esterhuizen, E., C. Mark, and M.M. Murphy. Numerical model calibration for simulating coal pillars, gob and overburden response. In *Proceeding of the 29th international conference on ground control in mining, Morgantown, WV*. 2010.

12. Mark, C. 1999. Introduction. In *Proceedings of the Second International Workshop on Coal Pillar Mechanics and Design, Vail, CO. 1999.* 2-3